

Supplementary Document of Revisiting Optimal Coding for I-ToF under Practical Sensor Constraints

Wenbin Luo Takafumi Iwaguchi
Kyushu University

Ryusuke Sagawa
DENSO IT Laboratory

Hiroshi Kawasaki
Kyushu University
kawasaki@ait.kyushu-u.ac.jp

S1. Exclusive Demodulation Mechanism

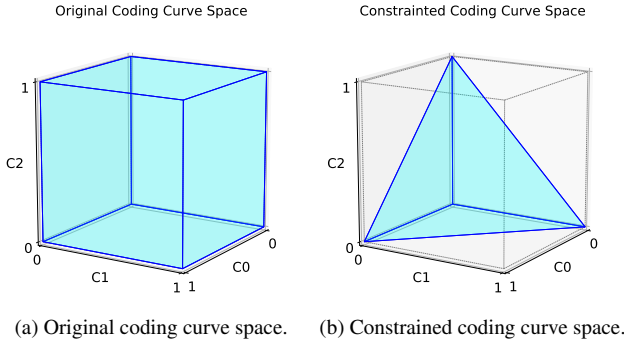


Figure S1. The original coding curve space and the one under exclusive demodulation mechanism.

In Sec. 4.1 of the main paper, we introduce an exclusive demodulation mechanism. This mechanism originates from multi-tap I-ToF, which usually avoids activating different taps simultaneously [1, 4] to prevent electrical crosstalk. In Eq. (22) of main paper, an equation about demodulation sequence is described to meet the exclusive mechanism in coding scheme design. In fact, we can also incorporate the exclusion mechanism into the coding curve space by combining Eq. (3) and Eq. (22):

$$0 \leq C_0(t) + C_1(t) + C_2(t) \leq 1. \quad (\text{S1})$$

And Eq. (S1) will limit the space of coding curve from original unit cube [2] to a regular tetrahedron as shown in Fig. S1.

This constraint will highly affect the performance of previous coding scheme. As shown in Fig. S2 (a), which illustrate the coding scheme with period 90 ns, ideal Hamiltonian coding curve [3] run along the edge of the unit cube. But in practical setting with exclusive demodulation, it will be converted to Fig. S2 (b), which use three times of period to achieve the same sensing range as (a). This makes the correlation 1/3 of ideal scheme and the coding curve length

also becomes 1/3 of original length and is limited into the regular tetrahedron space in Fig. S1b.

In Sec. 4.3 of the main paper, we compared different coding schemes with same laser peak power which leads to different total power. And we set same total power here to clearly show the influence of exclusive demodulation mechanism. As main paper, we set the integration time $T = 10$ ms, period $\tau = 90$ ns, albedo and light fall-off parameter $s = 0.01$ and readout noise standard variance $\sigma_r = 20$. But we set the laser power of proposed-high to $P_{max} = 1$ and power of Hamiltonian to $P_{max} = 2$, which bring us same total power $3.33e6$ for the two coding schemes.

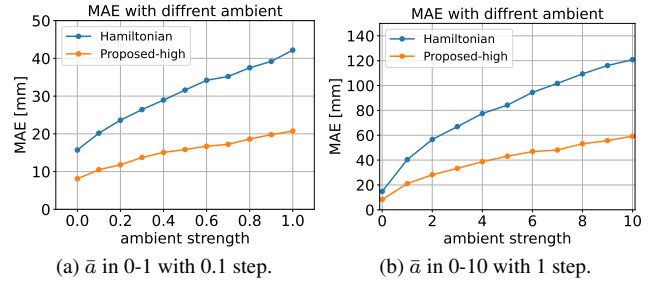


Figure S3. The result of MAE for Hamiltonian and proposed-high under different strength of ambient light with same total power in simulation.

The simulation result of MAE under different ambient strength is shown in Fig. S3. The power of ambient light is set to 0 ~ 1 with 0.1 step in Fig. S3a and 0 ~ 10 with 1 step in Fig. S3b. From the results, we can see that even with same total power, the Hamiltonian show worse MAE results than proposed-high due to the exclusive mechanism and their difference gets bigger with stronger ambient light. This demonstrates the crucial role of exclusion mechanisms, compelling us to consider them when designing coding schemes.

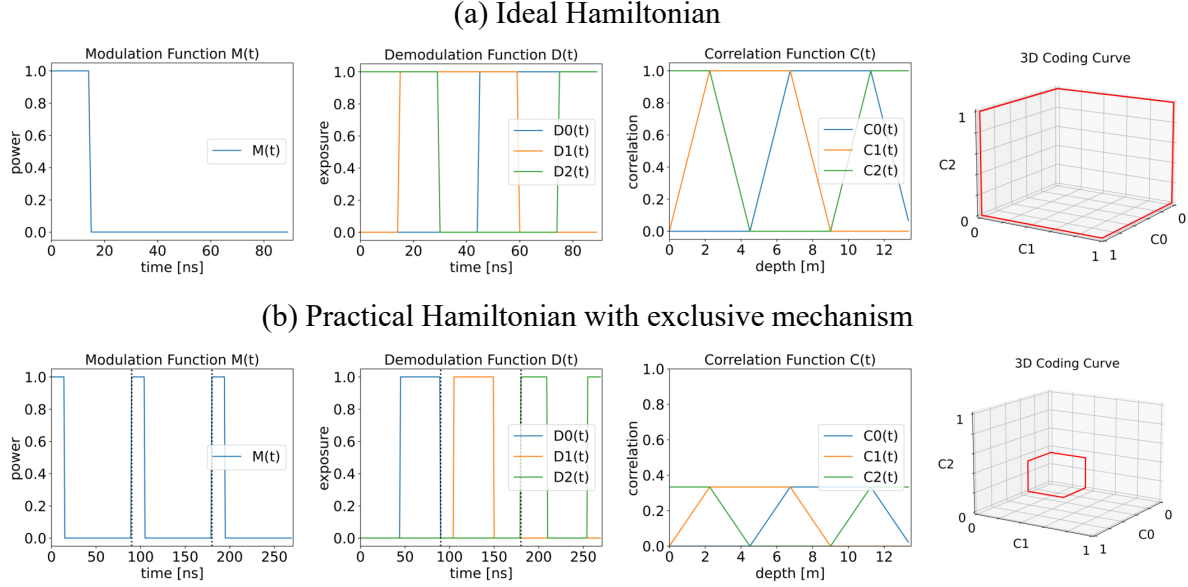


Figure S2. The coding schemes of (a) ideal Hamiltonian [3], (b) practical Hamiltonian with exclusive mechanism. The modulation, demodulation, correlation function and coding curve for every schemes are shown. Note that (b) have time range 3 times of period 90 ns in modulation/demodulation function due to exclusive mechanism.

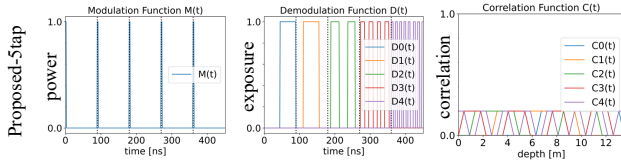


Figure S4. coding scheme for 5-tap Hamiltonian.

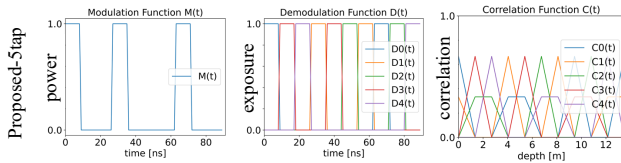


Figure S5. Found coding scheme for 5-tap.

S2. The simulation on multi-tap

In main paper, we use the three taps as example for the analysis, whose number is exactly same to the unknown parameters in depth estimation. But our work can also be extended to multi-tap (more than three) with just change the number if demodulation signals. And we use our method on 5-tap simulation with the same constraints and setting in main paper which set period 90 ns and integration time 10 ms with exclusivity, same laser power, binary and bandwidth.

The found coding scheme with high SNR setting is shown in Figure S5, which shown a complex correlation

Table S1. The Result of 5-tap simulation (mm)

coding scheme	MAE of high SNR	MAE of low SNR
Hamiltonian 3-tap	23.075	59.435
Hamiltonian 5-tap	15.954	122.188
Proposed 5-tap	3.165	7.351

function. The 5-tap Hamiltonian [3] is shown in Figure S4, which show very short laser opening time which is only 3 ns in 90 ns period, and it also need 5 times of periods time because of the exclusivity. And the simulation result compared to the 5-tap Hamiltonian is shown in Table S1 with low SNR and the setting of same laser power. Note that high/low SNR means the \hat{a} is set to 0 and 1.

From the result, we can see that 5-tap Hamiltonian with same laser power show improvement with high SNR setting than 3-tap, but it inversely show worse result in low SNR due to its extreme short time of laser opening. And proposed method show both big improvement on MAE result in high/low SNR setting than 3-tap and 5-tap Hamiltonian with our device constraints.

S3. The simulation without exclusivity

We also use our optimization method without exclusivity constraint, but relaxing exclusivity is possible by dividing the max laser power by the number of shared taps under the fixed total power constraint with thinking the structure of sensor. We performed the optimization using SA in non-

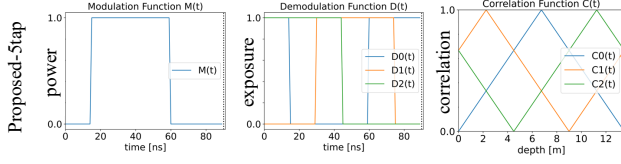


Figure S6. Found coding scheme for non-exclusive 3-tap.

Table S2. The Result of non-exclusvie simulation (mm)

coding scheme	MAE of high SNR	MAE of low SNR
Hamiltonian exclusive	23.075	59.435
Hamiltonian non-exclusive	23.200	99.428
Proposed low exclusive	9.353	18.005
Proposed low non-exclusive	18.098	48.330

exclusive 3-tap due to exponential complexity of 3 non-exclusive demodulation function, and the result with low SNR setting is shown in Figure S6.

And the simulation result with 90 ns period and 10 ms integration time is shown in Table S2. The non-exclusive Hamiltonian show close result to exclusive Hamiltonian in high SNR, but in low SNR, it show worse result because its lower laser power to achieve non-exclusivity. But proposed methods show better MAE result in high/low SNR both exclusive and non-exclusive than Hamiltonian. But non-exclusive result show worse result because its lower laser power and it can not be said as optimal one with SA optimization rather than brute-force in exclusive setting. But the results still show the effect of proposed optimization method and its feasible property on different problem setting, which means our framework can be extended to different structures of I-ToF.

References

- [1] Cyrus Bamji, John Godbaz, Minseok Oh, Swati Mehta, Andrew Payne, Sergio Ortiz, Satyadev Nagaraja, Travis Perry, and Barry Thompson. A review of indirect time-of-flight technologies. *IEEE Transactions on Electron Devices*, 69(6): 2779–2793, 2022. 1
- [2] Mohit Gupta, Andreas Velten, Shree K. Nayar, and Eric Breitenbach. What are optimal coding functions for time-of-flight imaging? *ACM Trans. Graph.*, 37(2), 2018. 1
- [3] Felipe Gutierrez-Barragan, Syed Azer Reza, Andreas Velten, and Mohit Gupta. Practical coding function design for time-of-flight imaging. In *Proceedings of the IEEE/CVF Conference on Computer Vision and Pattern Recognition (CVPR)*, 2019. 1, 2
- [4] Ryosuke Miyazawa, Yuya Shirakawa, Kamel Mars, Keita Yasutomi, Keiichiro Kagawa, Satoshi Aoyama, and Shoji Kawahito. A time-of-flight image sensor using 8-tap p-n junction demodulator pixels. *Sensors*, 23(8), 2023. 1